HHS Public Access

Author manuscript

Nat Chem Biol. Author manuscript; available in PMC 2011 May 01.

Published in final edited form as:

Nat Chem Biol. 2010 November ; 6(11): 797–799. doi:10.1038/nchembio.440.

The Structure and Mechanism of the *Mycobacterium tuberculosis* Cyclodityrosine Synthetase

Matthew W. Vetting[*], **Subray S. Hegde**[*], and **John S. Blanchard**[†]

Department of Biochemistry, Albert Einstein College of Medicine, 1300 Morris Park Avenue, Bronx, NY 10461

Abstract

The *Mycobacterium tuberculosis* enzyme Rv2275 catalyzes the formation of cyclo(L-Tyr-L-Tyr) using two molecules of Tyr-tRNA^{Tyr} as substrates. The three-dimensional structure of Rv2275 was determined to 2.0 Å resolution, revealing that Rv2275 is structurally related to the class Ic aminoacyl-tRNA-synthetase family of enzymes. Mutagenesis and radioactive labeling suggests a covalent intermediate in which L-tyrosine is transferred from Tyr-tRNA^{Tyr} to an active site serine (S88) by transesterification and with E233 serving as a critical base catalyzing dipeptide bond formation.

Cyclodipeptides (CDPs) and their diketopiperazine (DKP) derivatives are a large group of secondary metabolites that are produced predominately by microorganisms. Many complex DKP derivatives have received attention in recent years due to their diverse biological activities, including antibacterial (bicyclomycin, albonoursin), antifungal (cyclo(L-Phe-L-Pro), cyclo(L-Phe-trans-4-OH-L-Pro)) and antitumor (phenylahistin, ambewelamides A and B) activities[1–4]. In all cases except albonoursin biosynthesis, the synthesis of the DKP scaffold is catalyzed by nonribosomal peptide synthases (NRPSs) either by dedicated NRPSs or as truncated products of larger peptide synthesis clusters[5–8].

It was recently reported that the *Streptomyces noursei* protein AlbC catalyzes the formation of the albonoursin cyclodipeptide precursor cyclo(L-Phe-L-Leu) (cFL) using aminoacyl-tRNAs[9]. AlbC is a 239-residue polypeptide that is unrelated not only to NRPSs but also to all other structurally and functionally characterized proteins. *In silico* analysis of gene databases identified 7 other proteins exhibiting sequence similarity to AlbC. *Mycobacterium*

[†]Corresponding author: phone: (718) 430-3096, Fax: (718) 430-8565 blanchar@aecom.yu.edu.

[*]Both authors contributed equally to this work

[*]The atomic coordinates and the structure factors have been deposited in the Protein Data Bank, www.rcsb.org (PDB ID code 2x9q)

COMPETING INTEREST STATEMENT

The authors declare no competing financial interests

Note: Supplementary information is available on the Nature Chemical Biology website.

AUTHOR CONTRIBUTIONS

S.H. and M.V. contributed equally to this work and are listed as co-first authors. Funding was obtained by J.B. Experiments were conceived and designed by S.H., M.V. and J.B. S.H. cloned and purified Rv2275 and *Ec*TyrRS, performed the kinetic analysis, and did the radiolabeling experiments. M.V. determined the three-dimensional structure of Rv2275, and cloned and purified the Rv2275 mutants. The manuscript was drafted by S.H. and M.V. and revised by all authors.

tuberculosis has a chromosomally encoded AlbC homolog (Rv2275) exhibiting 26% sequence identity to AlbC. Recombinant *M. tuberculosis* Rv2275 catalyzed the Tyr-tRNA-dependent formation of cYY in *E. coli* cell lysates[9]. In *M. tuberculosis*, the adjacent gene encodes a cytochrome P450 (Rv2276) that catalyzes C-C bond formation between the carbons ortho to the phenolic hydroxyl of cYY, producing what we term mycocyclosin (Fig. 1a)[10]. Rv2276 was found to be an essential *M. tuberculosis* gene and it was suggested that either mycocyclosin was essential, or that the overproduction of cYY is toxic[10,11].

The crystal structure of Rv2275 was solved at a resolution of 2.0 Å (Supplementary Table 1,2; Supplementary methods). The structural model consists of the entire Rv2275 sequence minus forty-eight N-terminal residues (1–48), five C-terminal residues (285–289) and a loop between α6 and α7 (residues 212–216), which were not observed in electron density maps. Rv2275 exhibits a single domain 3-layer βαβ structure with a Rossmann fold (Fig. 1b; Supplementary Fig. 1). The core consists of a mostly parallel β-sheet bound on either side by helices. A structural homology search by secondary-structure matching (SSM)[12] identified Rv2275 as being structurally similar to the catalytic domains of tyrosyl and tryptophanyl-tRNA synthetases (class-Ic aa-tRNA synthetases). The top scoring result was the tyrosyl-tRNA synthetases from *Methanococcus jannaschii* (MjTyrRS; PDBID=1J1U)[13], with an r.m.s.d of 3.24 Å over 167 matched Cα positions, and 10% sequence identity (Fig. 1c). Rv2275 lacks the anticodon recognition domain typically found in aa-tRNA synthetases. Both Rv2275 and class Ic tRNA-synthetases are dimers, however they have significantly different dimer interfaces (Supplementary Fig 2).

Class I aa-tRNA synthetases contain an N-terminally located HIGH sequence that interacts with ATP. The HIGH sequence motif is located at the β2/α3 loop in an “open” conformation, held by interactions with α5. In Rv2275, the corresponding loop (β3/α2) lacks the same interactions with the corresponding helix but instead folds back on itself, with N91, Y93 and F94 completely occupying the position corresponding to the ATP binding site (Fig. 1b; Supplementary Fig. 3). These interactions are most likely essential to the CDPS active site architecture, as the position and interaction of two crucial catalytic residues, S88 (β3/α2 loop) and Y253 (β6) (see below) are strongly influenced by the conformation of the β3/α2 loop.

There is very low sequence identity between the members of the CDPS family, with most exhibiting less than 30% overall sequence identity (Supplementary Fig. 4). Six of the twelve completely conserved residues are clustered near a surface accessible pocket that roughly corresponds to the amino acid binding pocket of class I aa-tRNA synthetases (Fig. 1d). With the exception of Y253, all of the strictly conserved pocket residues are contained within the two consensus CDPS sequences, H^{82}x[LVI][LVI]G^{86}[LVI]S^{88} and Y^{229}[LVI]xxE^{233}xP^{235} identified earlier[9]. The base of the pocket consists of mostly hydrophobic residues (V84, G86, M170, L236, F237) with the exception of N251. Most of the strictly conserved residues in the substrate-binding pocket (G86, S88, Y229, E233, P235 and Y253) are arranged in two distinct clusters about the entrance to the hydrophobic pocket. On one side, S88 from the β3/α2 loop is hydrogen bonded (2.6 Å) to the side chain hydroxyl of Y253, while on the opposite side the side chains of Y229 and E233 project into the entrance (Fig 1d).

Determination of a CDPS crystal structure and localization of putative active site residues facilitates an examination of the CDPS mechanism. Since CDPSs utilize charged tRNA substrates, the enzymes must somehow co-localize two activated amino acids. One possibility is the binding of more than one charged tRNA per CDPSs subunit, with the enzyme catalyzing the formation of a dipeptide intermediate which then cyclizes. A second possibility is that the charged-tRNAs bind to a single site consecutively, with the first charged amino acid passed to an enzyme group by transesterification followed by release of tRNA. The second charged tRNA could then bind the same enzyme surface, followed by formation of dipeptide on the enzyme or the second tRNA.

To test these two possibilities enzyme kinetics and radioactive tagging experiments were performed. Firstly, kinetic parameters were determined for our Rv2275 enzyme preparation. Incubation of Rv2275 with L-Tyr, Tyr-tRNA, *Ec*TyrRS, ATP and $MgCl_2$ yielded cYY in a time dependent manner (Supplementary Fig. 5a) as previously observed [9]. Rv2275 exhibited a K_m value of 3.6 ± 0.3 μM for *E. coli* Tyr-tRNA^{Tyr} and a turnover number of 2.50 ± 0.06 s^{-1} (Supplementary Fig. 5b). The kinetic parameters, particularly the k_{cat}/K_m value observed here (0.7×10^6 M^{-1} sec^{-1}) is comparable to the k_{cat}/K_m value of LvFemX (0.73×10^6 M^{-1} sec^{-1}) for *E. coli* Ala-tRNA^{Ala}, an aa-tRNA dependent nonribosomal peptidyltransferase for which the kinetic parameters are known[14].

Rv2275 was then incubated with substoichiometric amounts of [^{14}C]-Tyr-tRNA^{Tyr} and the reaction mixture was fractionated by anion exchange HPLC to separate tRNA from Rv2275. Approximately 25% of the radiolabel coeluted with the protein (Fig. 2a), consistent with the formation of a covalent tyrosinoylated enzyme intermediate that is trapped under these conditions. Examination of strictly conserved residues suggested S88 as the likely nucleophile due to its relatively short hydrogen bond (2.6 Å) with the hydroxyl of Y253. Assays using the S88A mutant showed a complete loss of cYY-forming activity, and an abolition of protein radiolabeling (Fig. 2a; Supplementary Table 3).

Several additional mutants were made to examine the roles of conserved residues and to ensure that S88 was indeed the point of covalent attachment. The Y253F mutant retained a small but detectable amount of catalytic activity (200 fold decrease) consistent with the likely role Y253 plays in positioning and increasing the nucleophilicity of the S88 hydroxyl. The Y229F mutant only decreased in activity 20 fold, suggesting the phenolic hydroxyl plays a role in substrate binding. Both the E233A and the E233Q mutants demonstrated a complete loss of cYY-forming activity. The isosteric E233Q mutant was examined for retention of the covalent intermediate by HPLC (Fig. 2a). The E233Q mutant retained about 55% of the radiolabel amounting to approximately twice as much radiolabel as wild type. These results argue that E233 is not the point of covalent attachment and may play a role in the collapse of the tyrosyl-enzyme ester intermediate. The presence of the early peak (Tyr) in catalytically incompetent S88A and E233Q mutants is due to the hydrolytic instability of aminoacyl-tRNA.

We confirmed the presence of a covalently bound intermediate by isolating the tyrosyl-enzyme intermediate under two different denaturing conditions. In the first, substoichiometric amounts of [^{14}C]Tyr-tRNA^{Tyr} was mixed with WT Rv2275, E233Q and

S88A mutants and the proteins were separated on SDS-PAGE and autoradiographed. Radioactivity is clearly visible associated with WT Rv2275, while the E233Q mutant retained a higher amount of the radiolabel and S88A did not retain any radiolabel (Fig 2b). In a second experiment, His_6 tagged WT and mutant proteins were similarly radiolabled and bound to Ni-NTA beads. Beads were repeatedly washed with 5M urea. Denatured protein was eluted with imidazole and the radioactivity in the fractions was measured. No radioactivity above background was detected in the imidazole eluate of the S88A mutant. The WT Rv2275 and the E233Q mutant retained 3% and 15% of the total radioactivity, respectively (Supplementary Fig. 6). These results confirm the presence of a covalently bound tyrosyl-enzyme intermediate and S88 as the point of covalent attachment.

Based on the structure and our mutational analysis we propose catalysis occurs with the initial binding of Tyr-$tRNA^{Tyr}$ in an orientation such that α-amino group of tyrosine is positioned to allow for interaction with E233 (Fig. 3a). Nucleophilic attack by the S88 hydroxyl on the ester carbonyl results in the formation of the covalently tyrosinoylated enzyme and free Tyr-tRNA (Fig. 3b). In order for a second Tyr-$tRNA^{Tyr}$ to bind, the covalently bound tyrosine must swing out of its original binding pocket and the rotation of the side chain of S88 (from chi 1 = 55° to chi1 = 178°) would place the tyrosine in a large secondary surface depression (Supplementary Fig. 7). The formation of radiolabled tyrosinoylated enzyme with the E233Q mutant form of Rv2275 suggests that this initial transesterification chemistry does not require E233. The second Tyr-$tRNA^{Tyr}$ binds and the chemistry here becomes ambiguous. The α-amino group of the enzyme-bound tyrosine could attack the carbonyl ester of the Tyr-$tRNA^{Tyr}$ to generate the enzyme-bound dipeptide or the α-amino group of the tRNA-bound tyrosine could attack the enzyme bound tyrosine to generate the tRNA-bound dipeptide. The structure suggests that the latter is more likely, given the need for a general base to deprotonate the α-amino group to attack the enzyme ester bond. Once the first peptide bond is formed, the second chemical step occurs, and in this step E233 could assist in protonating the product 3′-hydroxyl group of tRNA. It is unclear how the protein plays a role in orienting the dipeptide to promote this cyclization chemistry, and although the intramolecular cyclization of a dipeptide ester is facile, it requires that the dipeptide be in a *cis* conformation to place the amine in proximity to the ester[15,16].

In conclusion, the structural determination of Rv2275 is the first of a member of the cyclodipeptide synthetase family and unexpectedly resembles the catalytic domain of class I tRNA-synthetases. However, Rv2275 lacks an ATP binding site, an anticodon binding domain and exhibits a different dimerization interface. The reaction proceeds via a ping-pong kinetic mechanism with a unique intermediate produced by an aminoacyl transesterification reaction. Future structural and bioinformatics studies may shed light on the nature of their evolution; did they evolve from fully functional tRNA-synthetases by losing features, or do they represent a divergence from a common primitive tRNA synthetase ancestor?

Supplementary Material

Refer to Web version on PubMed Central for supplementary material.

Acknowledgments

We thank Dr. David Soriano Del Amo and Myrasol Callaway of the Albert Einstein College of Medicine for their help in cYY synthesis and ESI mass spectrometry, respectively. This work was supported by National Institutes of Health Grant A133696.

Abbreviations

aa-tRNA	aminoacyl tRNA
aminoacyl-tRNA synthetases	aa-tRNA synthetases
CDPS	cyclodipeptide synthetase
cYY	cyclo(L-Tyr-L-Tyr)
DKP	diketopiperazine
***Ec*TyrRS**	*Escherichia coli* Tyrosyl-tRNA synthetase
***Mj*TyrRS**	*Methanococcus jannaschii* Tyrosyl-tRNA synthetase
NRPS	nonribosomal peptide synthases
TyrRS	Tyrosyl-tRNA synthetase

References

1. Nishida M, Mine Y, Matsubara T, Goto S, Kuwahara S. Bicyclomycin, a new antibiotic. 3. In vitro and in vivo antimicrobial activity. Journal of Antibiotics (Tokyo). 1972; 25:582–593.
2. Fukushima K, Yazawa K, Arai T. Biological activities of albonoursin. Journal of Antibiotics (Tokyo). 1973; 26:175–176.
3. Strom K, Sjogren J, Broberg A, Schnurer J. *Lactobacillus plantarum* MiLAB 393 produces the antifungal cyclic dipeptides cyclo(L-Phe-L-Pro) and cyclo(L-Phe-trans-4-OH-L-Pro) and 3-phenyllactic acid. Applied and Environmental Microbiology. 2002; 68:4322–4327. [PubMed: 12200282]
4. Kanoh K, et al. Antitumor activity of phenylahistin in vitro and in vivo. Bioscience, Biotechnology and Biochemistry. 1999; 63:1130–1133.
5. Balibar CJ, Walsh CT. GliP, a multimodular nonribosomal peptide synthetase in *Aspergillus fumigatus*, makes the diketopiperazine scaffold of gliotoxin. Biochemistry. 2006; 45:15029–15038. [PubMed: 17154540]
6. Gardiner DM, Cozijnsen AJ, Wilson LM, Pedras MS, Howlett BJ. The sirodesmin biosynthetic gene cluster of the plant pathogenic fungus *Leptosphaeria maculans*. Molecular Microbiology. 2004; 53:1307–1318. [PubMed: 15387811]
7. Gardiner DM, Howlett BJ. Bioinformatic and expression analysis of the putative gliotoxin biosynthetic gene cluster of *Aspergillus fumigatus*. FEMS Microbiology Letters. 2005; 248:241–248. [PubMed: 15979823]
8. Schwarzer D, Mootz HD, Marahiel MA. Exploring the impact of different thioesterase domains for the design of hybrid peptide synthetases. Chemistry and Biology. 2001; 8:997–1010. [PubMed: 11590023]
9. Gondry M, et al. Cyclodipeptide synthases are a family of tRNA-dependent peptide bond-forming enzymes. Nature Chemical Biology. 2009; 5:414–420. [PubMed: 19430487]
10. Belin P, et al. Identification and structural basis of the reaction catalyzed by CYP121, an essential cytochrome P450 in Mycobacterium tuberculosis. Proc Natl Acad Sci U S A. 2009; 106:7426–7431. [PubMed: 19416919]

11. McLean KJ, et al. Characterization of active site structure in CYP121. A cytochrome P450 essential for viability of *Mycobacterium tuberculosis* H37Rv. Journal of Biological Chemistry. 2008; 283:33406–33416. [PubMed: 18818197]
12. Krissinel E, Henrick K. Secondary-structure matching (SSM), a new tool for fast protein structure alignment in three dimensions. Acta Crystallogr D Biol Crystallogr. 2004; D60:2256–2268. [PubMed: 15572779]
13. Kobayashi T, et al. Structural basis for orthogonal tRNA specificities of tyrosyl-tRNA synthetases for genetic code expansion. Nature Structural Biology. 2003; 10:425–432. [PubMed: 12754495]
14. Hegde SS, Blanchard JS. Kinetic and mechanistic characterization of recombinant *Lactobacillus viridescens* FemX (UDP-N-acetylmuramoyl pentapeptide-lysine N6-alanyltransferase). Journal of Biological Chemistry. 2003; 278:22861–22867. [PubMed: 12679335]
15. Purdie JE, Benoiton NL. Piperazinedione formation from esters of dipeptides containing glycine, alanine, and sarcosine: The kinetics in aqueous solution. Journal of the Chemical Society-Perkin Transactions. 1973; 2:1845–1852.
16. Steinberg SM, Bada JL. Peptide decomposition in the neutral pH region via the formation of diketopiperazines. Journal of Organic Chemistry. 1983; 48:2295–2298.

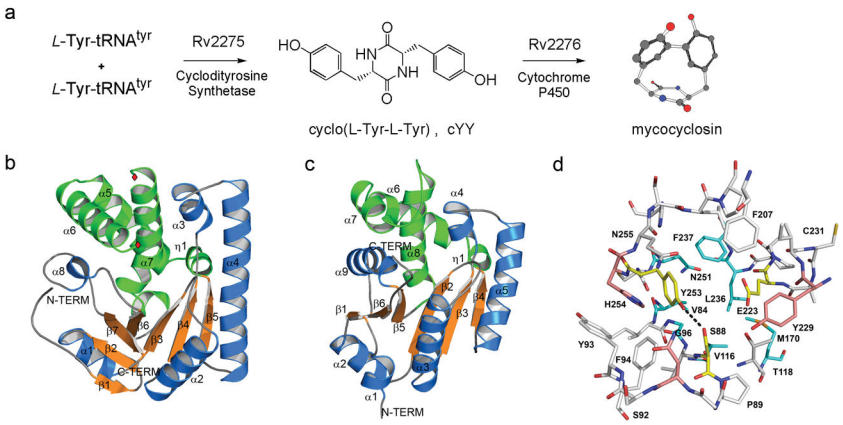

Figure 1. Cyclodityrosine synthetase reaction and 3-dimensional structure

(a) Reaction scheme for synthesis of cyclodityrosine in *Mycobacterium tuberculosis*. Ribbon diagrams of **(b)** Rv2275, **(c)** catalytic domain of *Mj*TyrRS. The terminal ends of a mobile loop not seen in the Rv2275 structure are labeled with red diamonds. The CP1 domain, a series of α helices located in the middle of the Rossmann fold of type I aa-tRNA synthetases, is colored green. **(d)** Stick diagram of residues around the two sequence motifs of CDPSs (H^{82}x[LVI][LVI]G^{86}[LVI]S^{88} and Y^{229}[LVI]xxE^{233}xP^{235}) and which are proposed to be involved in binding and catalysis. Residues at the base, the rim and the periphery of the pocket are colored with cyan, yellow, and salmon carbons respectively. A dotted line is shown to illustrate the hydrogen bond between S88 and Y253. **(e)** Model of the S88-tyrosyl ester with the tyrosyl group bound to the internal pocket, and S88 in its observed position. Tyrosine ester shown with yellow carbons and S88 with green carbons. Potential hydrogen bonds between E233, Y229 and the tyrosyl amide shown as dashes. The side chain of N251 is approximately 4.5 Å from the tyrosyl hydroxyl and therefore the dashed lines are for illustrative purposes only.

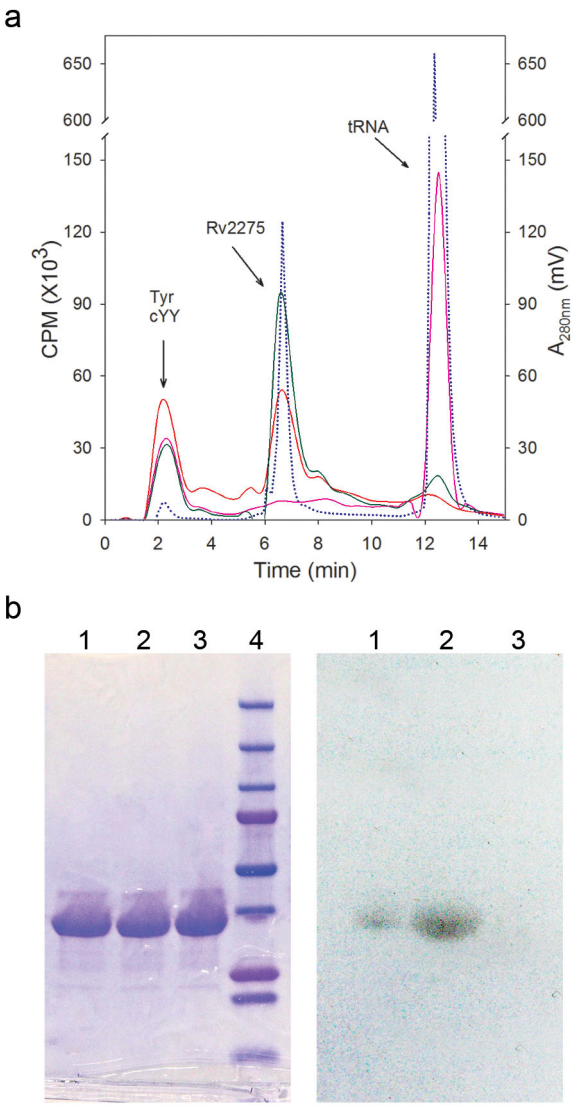

Figure 2. Visualization of acyl-enzyme intermediate

(a) Enzyme was mixed with [^{14}C]Tyr-tRNA^{Tyr} and separated by ion exchange chromatography as described in Methods. Radioactive counts (cpm) from individual experiments were overlaid; WT Rv2275 (orange), S88A (magenta), and E233Q mutants (green) along with A_{280} nm (dotted Blue) of the chromatogram. **(b)** Enzyme was mixed with [^{14}C]Tyr-tRNA^{Tyr}, separated on SDS-PAGE and autoradiographed as described in Supplementary Methods. Left panel is Coomassie blue stained SDS-gel. Lanes 1–3 are 20 μg - WT Rv2275, E233Q and S88A mutants, respectively; lane 4, molecular weight markers (top to bottom, 250, 150, 100, 75, 50, 37, 25, 20 and 15kDa). Right panel developed autoradiogram of 20 μg WT Rv2275 (lane 1), E233Q (lane 2) and S88A (lane 3) mutants, respectively.

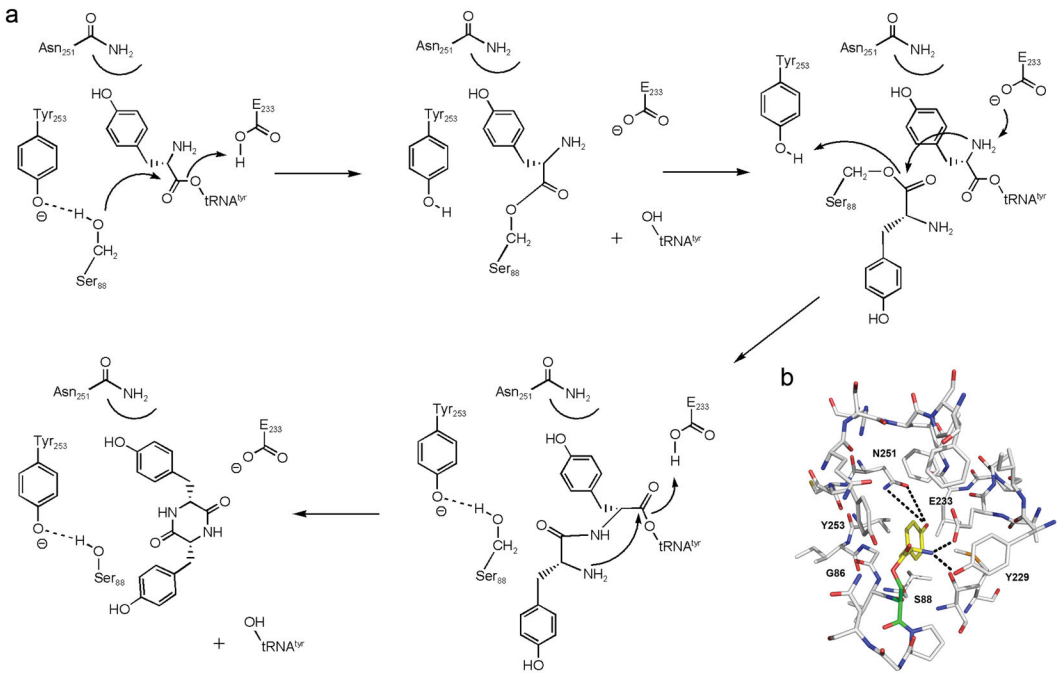

Figure 3. Proposed mechanism of cyclodipeptide formation for cyclodipeptide synthetases

Shown is the mechanism where the dipeptide ester is formed on the tRNA. An equivalent argument could be made for the formation of the dipeptide ester of S88, however the roles of the enzyme groups would not change.